Journal of Computational and Applied Mechanics, Vol. 2., No. 1., (2001) pp. 21–35

LARGE EDDY SIMULATION OF DISPERSION OF PARTICLES IN TURBULENT JETS

Zhilei Wu and Laszlo Fuchs
Division of Fluid Mechanics, Lund Institute of Technology
S-221 00 Lund, Sweden
Laszlo.Fuchs@vok.lth.se

[Received: January 15, 2001]

Abstract. The objective of this study is to closely investigate the interaction between turbulence and particles in a free jet. The round jet is loaded with heavy but small particles. The continuous phase is simulated using LES while particles are tracked using a Lagrangian (LPT) approach. The particle volume fraction is supposed to be small enough to exclude direct particle-particle interactions. We have also considered the case of one-way interaction in which the particles have no effect on the continuous phase turbulence. The effect of the large vortex ring structures on particle dispersion has been studied. Particles with Stokes numbers in the range 0.03 to 10 have been considered. The computed results have been compared to our simultaneous double PIV measurements. The computed and the experimental results show very good agreement for the spatially developing jet both in terms of mean quantities as well as in terms of the correlation between the fluctuating velocities of the two phases. For forced jets the phase averaged particle concentration field shows that particles of different sizes tend to form particle-size dependent regions with high particle concentrations.

Keywords: Multi-phase flows, turbulent dispersion, LES, jet flows

1. Introduction

Particle dispersion by turbulent shear flows is superficially a simple problem, yet it is very common, and, therefore, an interesting test-bed for experimental and numerical tools. In many industrial processes the instantaneous particle concentration contains more important information than the mean concentration. One such example is the mixing process of fuel particles/droplets injected into a combustion device. Due to non-linear effects, the average of the interactions does not equal the averages of the interactions. This difference has to be accounted for in the form of a model. Otherwise, a more straightforward approach could be handling the non-linearities by computing the time-dependent problem (using Large Eddy Simulations, LES) and from such data compute the averaged values that are of interest.

The relative importance of the presence of the particles in the flow can be estimated by considering the different time-scales of the problem. For small particles one may assume that their shape is spherical and the "slip-velocity" is small. With these assumptions the particle Reynolds number is so small that the flow is (almost) Stoksian from the particle point of view. Under such assumptions, the aerodynamic response time of a particle is given by $\tau_A = \rho_p d_p^2/18\mu$, where ρ_p is the particle density, d_p is the particle diameter and μ is the fluid viscosity. This quantity represents

the time-scale required for a particle to adjust its velocity to the (continuous phase) flow velocity. The characteristic time-scale of a flow is given by $\tau_F = \delta/U$, where δ is the characteristic length-scale and U is the characteristic velocity of the flow. For jets the flow time-scale (of the large scales) can be estimated by $\tau_F = D/U_0$, with D being the inlet diameter and U_0 the inlet center-line velocity of the jet. The extent of dispersion of particles in such a flow situation is then determined by the Stokes number, which is defined as the ratio of the two time-scales: $\gamma_\tau = \tau_A/\tau_F$. This non-dimensional number characterizes the ability of the particle to follow the fluid elements. For particles with Stokes numbers much greater than unity, i.e.. $\gamma_\tau >> 1$, the particles will not respond to the large scale structures of the flow while particles with Stokes numbers much less than unity, i.e. $\gamma_\tau << 1$, will adjust to flow field very rapidly and will follow the flow field. Particles with Stokes numbers around unity will only partially respond to the local flow conditions. Such particles also affect largely the flow itself.

Particle dispersion in turbulent flows has been studied experimentally by several researchers. Longmire and Eaton [1] studied the interaction of solid particles with a turbulent flow by examining particle dispersion in jets. In their work, the jet was forced acoustically to form large vortex-ring structures. They confirmed that local particle dispersion and concentration are governed by convection due to large-scale structures. Some particles become clustered in the saddle regions downstream of the vortex-rings while others are ejected away from the main stream of the flow. The phase-averaged (during the forcing cycles) results revealed the mechanisms for the formation of particle clusters and the dispersion of particles. The large-scale structures and convection mechanisms have been shown to persist for particle-to-air mass loading ratios up to 0.65. Longmire and Eaton [1] did not examine the effect of different Stokes numbers on the results. Kiger and Lasheras [2] have also done experiments to investigate particles dispersion by vortex parings. In their experiment, the shear layer was forced with a fundamental frequency and sub-harmonic perturbations. Their results show that the vortex-ring structures play a role in homogenizing the particle concentration field. However, the amount of homogenization is strongly dependent on the particle relaxation time, the eddy turn over time as well as the time that the particles interact with each scale prior to a paring event (i.e. "residence time"). Small particles will be dispersed homogeneously, but larger ones are dispersed in an inhomogeneous fashion. The above mentioned papers give a global understanding of how the particles interact with large vortex-ring structures. These papers lack, however, information about the effects of the initial conditions on the particles and on their dispersion. This aspect is addressed here.

Several numerical simulations have been done to investigate particle behavior in turbulent flow fields. Squires and Eaton [3] have investigated the preferential concentration of particles by turbulence. They use Direct Numerical Simulation (DNS) to simulate an isotropic turbulence and investigated the effect of turbulence on the concentration field of heavy particles. Their results show that heavy particles gather in low vorticity and high strain rate regions. This accumulation effect is most pronounced for particles with a Stokes number of around 0.15. Recent development has shown that particles are greatly dispersed by large-scale structures rather than

three-dimensional turbulence. Chung and Troutt [4] have simulated particle dispersion in an axi-symmetric air jet. They use the discrete vortex method to simulate the vortex-rings of the jet. In their simulations, particles with different particle Stokes numbers are released at the jet inlet with the speed of the fluid. The results show that particles with Stokes numbers around unity might be dispersed beyond the corresponding dispersion of a passive scalar. Numerical simulations have been carried out by different researchers using both DNS and LES applied to the continuous phase in different geometries. Uijttewaal and Oliemans [5] have simulated particle dispersion in a vertical pipe flow based on DNS solver for the continuous phase. They point out that the interaction between particles and turbulence, neglecting wall effects, can result in particle segregation. Marcu and Meiburg [6] simulated particle dispersion by the braid vortices in a plane mixing-layer. An analytical expression for the critical particle diameter below which accumulation is possible has been derived. Tang et al. [7] have investigated particle dispersion in a plane wake as well as the effect of particle dispersion patterns at different particle Stokes numbers. Tang et al. [7] have also pointed out that particles at Stokes numbers around unity will be mostly dispersed.

This paper is aimed at studying effects of particle initial conditions for the dispersion in unforced and forced jets. Further, we consider the effect of Stokes number on the dispersion. By using LES also the non-linear drag effects can be assessed.

2. Mathematical models

2.1. The flow field of the continuous phase. In our simulations, the turbulence of the continuous phase is modeled by Large Eddy Simulation (LES). In LES, the large turbulence scales are resolved directly, while the effect of scales smaller than the finest grid size are modeled. The dominant force acting on heavy particles is primarily the drag. Since the drag varies non-linearly with the "slip-velocity", it is reasonable to assume that these non-linear effects are neglected if the flow field is computed in the framework of the Reynolds Averaged Navier Stokes (RANS) equations. One may compensate for the non-linear drag effects by adding an additional model term to the mean equations. Currently, there exist no such models in the literature. Therefore, it is natural to work within the LES framework. By this approach one avoids the need for temporal averaging. On the other hand, one has to make a series of assumptions. First, we assume that the particles are spherical and that the mean distance between the particles is much larger than the particle diameters. We also assume that the mean distance among particles is larger than the small resolved scales and hence the dispersed phase cannot be considered as a continuum. The relatively large distance among the particles implies that one may neglect interaction among particles. Thus, with the assumptions made here we take into account only one- and two-way interactions. Thus, the individual particles are tracked independently of each other, assuming that the particles displace a negligible amount of fluid. As stated above, the main force that acts on the heavy spherical particles is the aerodynamic drag. A disturbing effect arises with the combination of LES with the Lagrangian approach for Stokes numbers of $O(1)$ (or larger). This is so since LES requires adequate spatial resolution. That resolution should be such that eddies of the size of the Taylor

micro-scale are resolved, i.e., the spatial resolution if then of $O(Re_T^{-1/2})$. For heavy particles ($\rho_p/\rho_f = O(10^3)$) and if the Stokes number is $O(1)$ or larger, then the particle diameter is not much smaller than the grid size in our calculations. In spite of this potential inconsistency we do assume in the following that the spherical particles do not displace fluid.

In LES, the space filtering of a function $f(x_i, t)$ is defined as:

$$\overline{f(x_i,t)} = \int_{-\infty}^{\infty} G(x_i - x_i^{'}) f(x_i^{'}, t) \mathrm{d}x_i^{'} \tag{2.1}$$

where G is a filter function.

Filtering the Navier-Stokes equations leads to the equations for the resolved variables $\bar{u}_i$ and $\overline{p}$. The filtered incompressible equations are as follows:

$$\frac{\partial \bar{u}_i}{\partial x_i} = 0 \tag{2.2}$$

$$\frac{\partial \bar{u}_i}{\partial t} + \bar{u}_j \frac{\partial \bar{u}_i}{\partial x_j} = -\frac{1}{\rho}\frac{\partial \overline{p}}{\partial x_i} + \nu \frac{\partial}{\partial x_j}\frac{\partial \bar{u}_i}{\partial x_j} - \frac{\partial \tau_{ij}}{\partial x_j} + \bar{F}_i \tag{2.3}$$

$$\tau_{ij} = \overline{u_i u_j} - \bar{u}_i \bar{u}_j \tag{2.4}$$

where $\bar{F}_i$ is a source term and τ_{ij} is the Sub-Grid-Scale (SGS) stress tensor which reflects the effect of unresolved scales on the resolved ones. The role of the SGS term includes dissipation of turbulent kinetic energy. Such dissipation is needed to prevent a build-up of turbulent kinetic energy on the small scales. Since the (mean) rate of transfer of energy from the large to the small scales is independent of viscosity in the inertial sub-range (Kolmogorovs theory), any form of viscosity will be adequate. The dissipative effects should, however, maintain the inertial sub-range intact (i.e. not too much dissipation). Hence, any dissipative numerical scheme which provides adequate *amount* of dissipation can play the role of the SGS, independent of its functional form. Of course, explicit SGS models can account for another role of the SGS term, namely backscatter. The energy cascade is uni-directional only in the average sense. Instantaneously, there may be localized energy transfer from the smaller eddies to the larger (resolved) one. Different SGS models can give rise to backscatter. Gullbrand and Fuchs [8] have studied the effects of several SGS models, including the "Divergence Dynamic Model", the "Scale Similarity Model" and the "Exact Differential Model". The effect of different SGS on mean quantities is important only for low resolution situations. The gain by a SGS model is equivalent to a computation on a refined grid (by a factor two in each direction) without any explicit SGS term. Therefore, in this paper, no explicit SGS model is applied.

2.2. Particle motion equation. Particles are tracked by a Lagrangian method assuming that the particles have the properties as stated above. The momentum equation for the particles satisfies:

$$m\frac{d\mathbf{u}}{dt} = \mathbf{F} \tag{2.5}$$

Where $\mathbf{F}$ is the force on the particle and m is its mass. The forces acting on a single particle are detailed in the expression by Maxey and Riley [9]. They identified

different components of the force: drag, added-mass, buoyancy and history term. For heavy particles in gas the primary component of this force is the drag. This has the form:

$$\mathbf{F} = \frac{1}{8}\pi d^2 \rho C_D \left|V_R\right| V_R \tag{2.6}$$

where the drag coefficient is given by:

$$C_D = 24(1 + 0.15Re^{0.687})/Re \tag{2.7}$$

The particle Reynolds number is defined:

$$Re = \rho V_R d/\mu \tag{2.8}$$

where, d is the particle diameter, ρ and μ are the density and viscosity of the continuous phase, V_R is the relative velocity of the particle relative to the surrounding fluid.

3. Numerical methods

The spatial discretization of the governing equations for the continuous flow field is performed on a uniform Cartesian staggered grid. Locally refined grids can be introduced where required for adequate resolution. The convective terms are discretized using hybrid scheme and higher (third- and fifth-) order can be achieved by deferred correction. A proof of this process is given in Gullbrand et al. [10]. The lower order scheme is used only during the relaxation procedure which maintains the global high order. The time derivatives are discretized using a three level second order implicit scheme. The discretized conservation equations are solved iteratively using a multi-grid method. The particles are tracked by integrating the equation of motion for the particles, based upon the instantaneous velocity field, using a second order Runge-Kutta scheme.

4. Problem description

We simulate a particle-laden turbulent jet. Large Eddy Simulation is used to simulate the continuous phase, while the individual particles are tracked. In the case of the forced jet it is excited with a frequency of 364 Hz. The round jet has an inlet diameter of 2 cm. The fluid (air) has a mean inlet velocity of 14.4 m/s, corresponding to a Reynolds number of 19000. The particles are released at inlet at each time step during the simulations. The rigid spherical particles have a density of 2400 kg/m^3. To assess the effects of different particle sizes we consider three classes of particle-Stokes numbers (γ_τ): $0.03, 1$ and 10, respectively. We also want to study the effects of particle velocity on the particle dispersion. Therefore, we consider three different inlet particle velocities (relative to the fluid). For each of these particle velocities, we consider the three particle groups. The computed cases are summarized in the following table:

Case 1	Case 2	Case 3
forced jet	forced jet	forced jet
$U_p = U_f$	$U_p = 0.75U_f$	$_p = 0.5U_f$
$\gamma_\tau = 0.03,1,10$	$\gamma_\tau = 0.03,1,10$	$\gamma_\tau = 0.03,1,10$

Here, U_p, U_f and γ_τ are the averaged particle inlet centerline velocity, averaged fluid inlet centerline velocity and particle Stokes number, respectively. The forced jet inlet velocity profile (of the fluid phase) as a function of time is as follows:

$$u_f(t) = 14.4 * (1 + 0.15 * \sin(2\pi\ 364\ t)) \tag{4.1}$$

At each time step, a group of particles is released at the jet inlet. The particles are randomly distributed at the inlet, which results in a statistically uniform distribution. Particles are specified with different inlet velocities to examine the influence of initial slip velocity on particle dispersion. No radial velocity is imposed on the particles, which may be quite different from the real experimental set-up. This ideal situation may be advantageous in understanding the interaction between the particles and the flow structures. Since we are interested in the particle dispersion by the continuous phase, we use a dilute system, which means that no particle-particle interaction will be taken into account. Due the low volume fraction, the particles are supposed to have no effect on the continuous phase. Thus, the results for the forced jet have been computed using mostly a one-way coupling. Two-way coupling has been used in some of the cases, such as those displayed in Figures 1-3.

5. Results and discussion

5.1. Model validation. First, we consider the flow of a turbulent jet at a Reynolds number of 5100. For this low Re we do not use any Sub-Grid-Scale term, since the fine grid computations are close to DNS. This case has also been studied by us

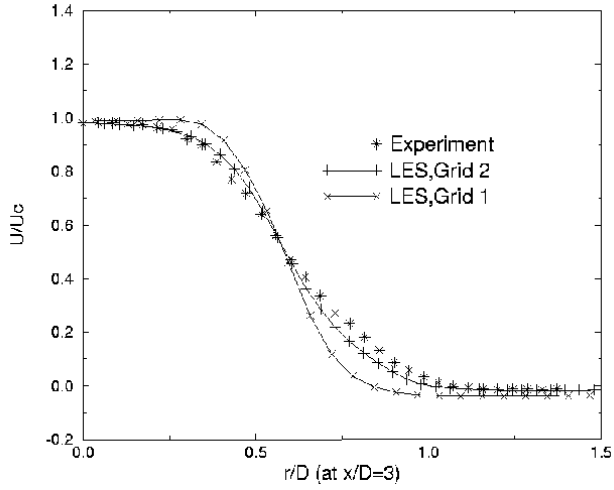

Figure 1. Fluid mean axial velocity at $x/D = 3$

experimentally by using an enhanced PIV system. The system allows one to measure simultaneously the velocity fields of both phases. This is done by using fluorescing tracer particles, while the Ni particles (sized around 165 μm) are measured directly. Figures 1 and 2 depict the mean velocity profiles of the two phases, respectively, at a distance of three jet diameters downstream of the nozzle. The figures compare the experimental results with those obtained by LES/LPT on two different grids (about 0.5 and 1.5 Million grid points, respectively). As seen, these quantities are captured quite well even on the coarser grid.

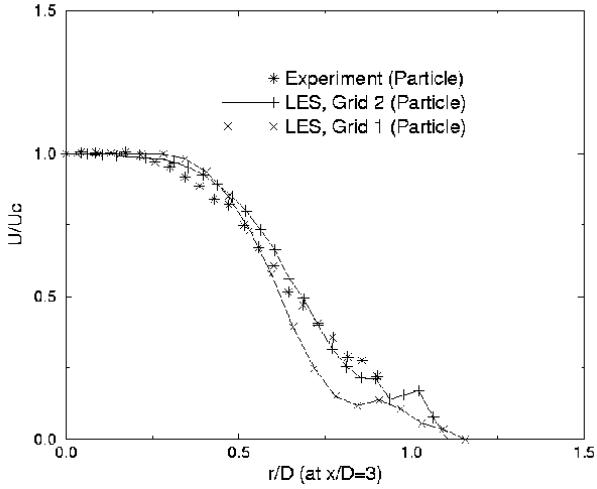

Figure 2. Mean axial velocity at $x/D = 3$ – particle phase

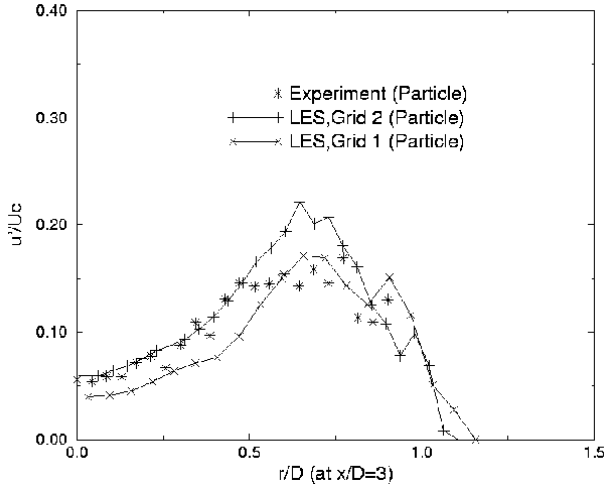

Figure 3. Mean axial velocity fluctuations, $x/D = 3$ – particle phase

The quality of the numerical results can be assessed better if one considers the fluctuating components. Figure 3. depicts the radial distribution of the axial velocity

fluctuations of the dispersed phase at a distance of three diameters form the nozzle exit. The non-smoothness of the results depends on the too low number of samples in the numerical and in particular in the experimental results.

For further validation, a case with the similar situation to that in [1] has been chosen. Simulation results are compared with those experiments.

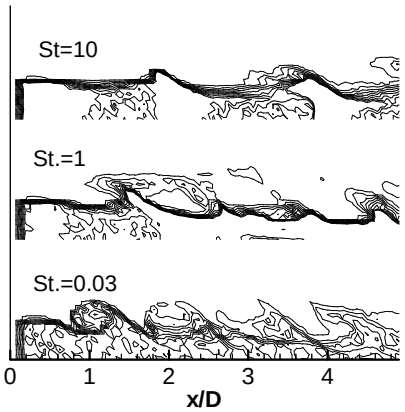

Figure 4. Phase average particle density map (Case 1)

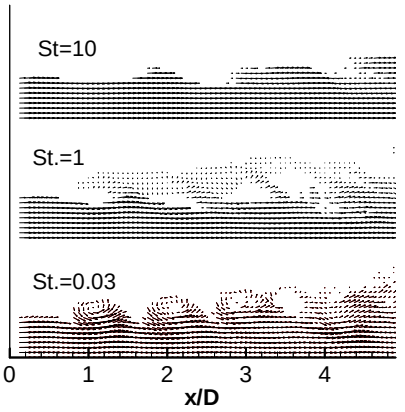

Figure 5. Phase averaged particle velocity field (Case 1)

First, we examine phase averaged particle and fluid properties qualitatively in the forced cases. The averages are obtained from a bin of phase angles of 1° centered at phase angle $\Phi = 0°$. For other phase angles, the pictures may be quite different, but to understand particle vortex-ring interaction, the results from any phase angle may be helpful and quite representative. Since large vortex-ring structures are only dominant in the proximal region of the jet, we present the result from jet inlet up to around 5 inlet diameters distance downstream.

Figures 4 and 5 correspond to Case 1. The figures show only a half plane due to the axi-symmetry of the phase averaged data. In this case, particles are released at each time step with the same velocity as that of the local fluid. Figure 4 is the phase averaged particle concentration field and Figure 5 is the corresponding phase averaged particle velocity vector field. Particles with Stokes number of 0.03 adjust to the fluid very quickly and follow the fluid motion quite well. Thus, the phase averaged concentration field clearly outlines the large vortex-ring structures. But even particles with such small Stokes numbers can not follow the fluid motion exactly. As these particles move downstream, they are thrown outwards slightly by the vortex-ring structures, which results in a "source" region in the vector field at about 3.6 inlet diameters downstream (Figure 5). When particle Stokes number is about unity, the particle responds to the fluid flow so that at the vortex-rings the particles follow a curved path. However, due to the particles' own inertia, they cannot follow the vortex-ring exactly and are thrown away from the center region of the vortex by the centrifugal force. Particles which are originally located at the outer region of the large vortex-ring structures may be just ejected away form the main stream, while

other particles may be dragged back to the main stream again. In the vortex core region, there are no particles left. Since some particles are ejected away from the main stream, they will show up in a region outside of the jet resulting in a wider particle dispersion than the corresponding single phase jet. This can be seen both from the concentration field and from the velocity vector field. Particles with a Stokes number of 10 are only displaced slightly compared to those with Stokes numbers of 0.03 and 1. The phase averaged concentration map of these particles is distorted a little and the distortion of the particle concentration field does not follow the fluid vortex paring events. From the above we note that when the particles at the inlet have the same velocity as the fluid, the particles with Stokes number of 1 exhibit the strongest dispersion pattern. Particles with

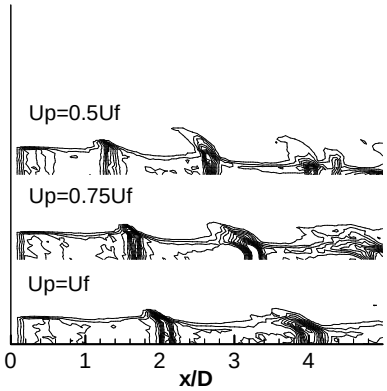

Figure 6. Phase averaged particle density map for different particle inlet velocities ($\gamma_\tau = 10$)

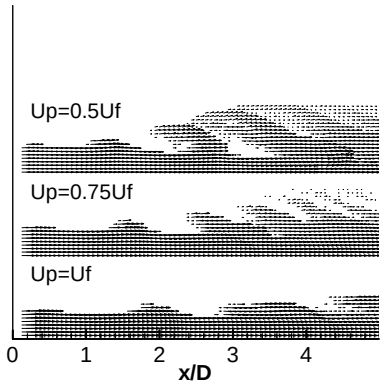

Figure 7. Phase averaged particle velocity field ($\gamma_\tau = 10$)

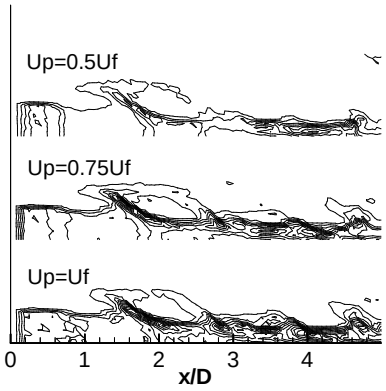

Figure 8. Phase averaged particle density map ($\gamma_\tau = 1$)

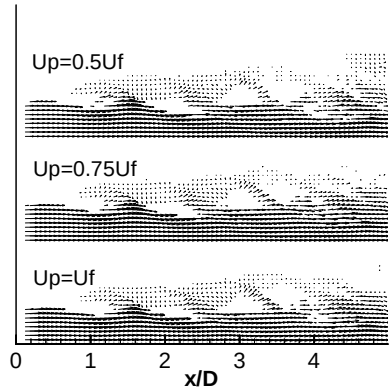

Figure 9. Phase averaged particle velocity field ($\gamma_\tau = 1$)

Stokes number of 10 will respond only slightly to the fluid and be hardly dispersed. Particles with Stokes number of 0.03 will follow the fluid motion quite well and will

not be dispersed much beyond that of the single phase turbulent jet.

Next, we consider the effects of particle slip velocity at the inlet. Particles of the same size are released at the inlet with different inlet velocity i.e., particles take 100%, 75%, and 50% of the local fluid velocity. Figures 6, 7 and 8, 9 correspond to particles of Stokes numbers of 10 and 1, respectively. For particles with Stokes number of 10, it is quite clear that different initial velocity changes the particle dispersion pattern and the particle velocity field dramatically. When particles initially take the same velocity as the fluid, they are only slightly dispersed by the vortex-ring structures. In this case the particles are clustered in "pockets" traveling downstream. The interval among the clusters is quite large compared to that of the vortex-rings. As the particle initial velocities are reduced, particles are dispersed further and further and the interval between particle clusters becomes smaller and smaller. As the particles initial velocity is decreased, the "tail" of the particle clusters become more and more clear. This behavior can be explained rather easily. When the particles have small velocities they have longer time to interact with the vortex-ring structures, leading to a stronger dispersion than those particles which have a smaller slip velocity. For particles with Stokes number of 1, different initial velocities do not have that much effect on the particle dispersion pattern and hence the extent of particle dispersion. Even though particles are released at the inlet with different velocities, they exhibit clusters at the same axial positions, with the same spacing (around 1 D) among the clusters. This is clearly seen in Figures 8 and 9. For particles with Stokes number of 0.03, different initial velocities have even smaller effect on the particle dispersion pattern. This behavior is rather obvious since the smaller the Stokes number is, the quicker the particle will adjust to the surrounding flow conditions. From these results we can draw the conclusion that as far as these jet cases are concerned, when the particle Stokes number is larger than unity, the particle nozzle slip-velocity, $(U_f - U_p)$, plays an important role in the particle dispersion. In this case, the larger the nozzle slip-velocity is, the greater the particle dispersion is.

In order to determine how fast particles are moving in the flow field and also to determine how the mean of particle concentrations differs under different situations, time averaged particle velocity and particle concentration fields are presented in quantitative terms.

5.2. Statistical results. Mean properties. Consider Cases 1 and 3 where the forced jet is loaded with particles of different Stokes numbers. Figures 10 to 13 depict the particle axial velocity and the particle radial velocity at different axial positions. For particles with Stokes numbers of 0.03 and 1, the particle axial velocity decreases rather quickly at $r = 0.25D$, while for particles with Stokes number of 10, particle axial velocity begins to decrease only after $r = 0.5D$. The higher momentum of the larger particles is maintained until $r = 0.65D$. This is due to the larger inertia of those particles. It is interesting to note that the radial velocity at this axial station (Figure 11) is pointing towards the center for $r = 0.5D$. This is so in particular for $\gamma_\tau = 1$. However, as these particles get closer to the jet axis they gain axial velocity (from the fluid) and therefore tend to disperse with it. Altogether, these two counteracting mechanisms lead to an off-axial peak of particle number density (c.f. Figure 15) for the larger particles. The largest effect is noted for particles with

$\gamma_\tau = 1$. The smallest particles follow the fluid and disperse with it and therefore no such effects are observed. These effects have also been observed by Longmire and Eaton [1] experimentally. Their explanation was, however, that the particles gained negative radial velocity as they passed through the jet nozzle. However, in our current simulation, no radial velocities are specified for the particles at jet inlet. Combined with the phase averaged results shown in Figures 4 to 9, we may attribute this negative velocity to the particle-vortex interaction. When the vortex-rings developed and move downstream, they drag the particles with themselves. The motion of the individual particles depends upon the position of the particle relative to the core of the vortex.

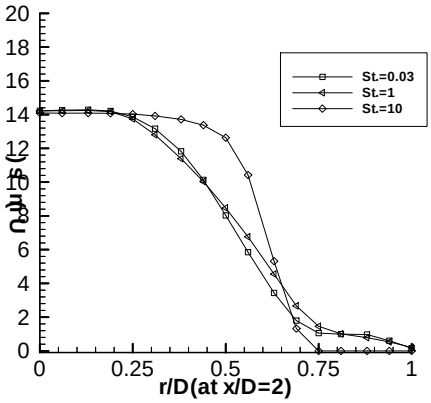

Figure 10. Averaged particle axial velocity at $x/D = 2$

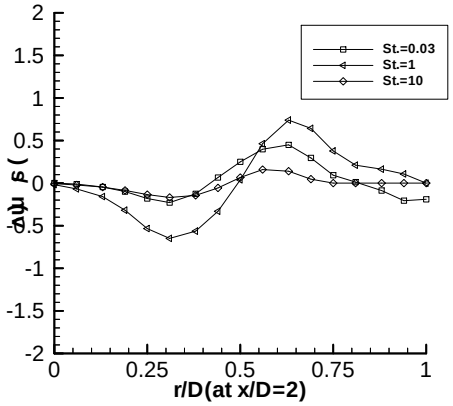

Figure 11. Averaged particle axial velocity at $x/D = 4$

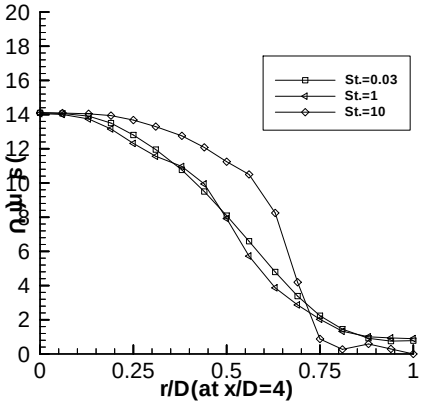

Figure 12. Averaged particle radial velocity at $x/D = 2$

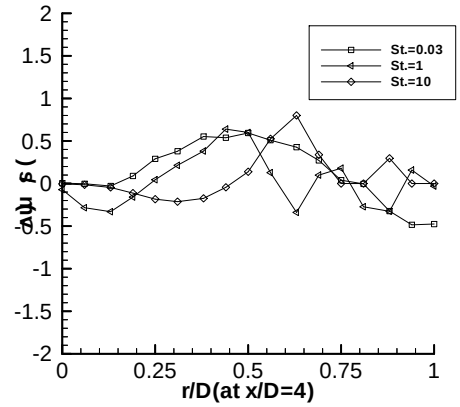

Figure 13. Averaged particle radial velocity at $x/D = 4$

Particles with Stokes number 1 gain the largest negative radial velocity in the main stream region and the largest positive velocity outside the main stream, this is most

clearly seen at $x = 2D$ (Figure 11). This is reasonable since particles with the medium Stokes number have moderate inertia to maintain their speed, while they are also light enough to be responsive to the local flow structure. It is interesting to note that the mean particle radial-velocity highly depends on the Stokes number. In Figures 11 and 13 we note that the radial velocity component changes sign. This implies that on average an even particle distribution at the inlet will lead to non-homogenous distribution later downstream. This is reflected also in the particle number densities. The fact that particles with Stokes number around unity disperse mostly is seen also in the radial velocity component. These particles may have positive and negative radial velocity directions. The smaller particles follow the fluid better and therefore have also a more monotonous particle number density distribution. The larger particles ($\gamma_\tau = 10$) are heavier and hence inertia dominates. Due to inertia, the particle motion of the individual particles will be rather complex. This observation supports the idea that non-linear effects (also in terms of the drag force) make simpler, linear type models for describing the interaction between the phases highly non-general.

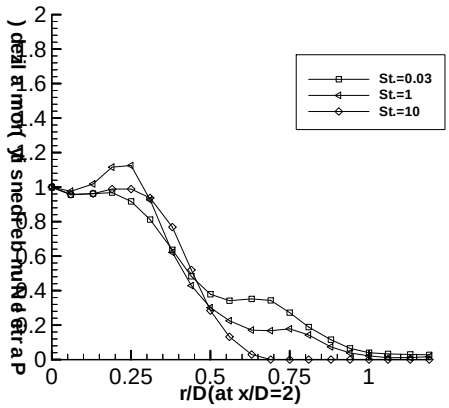

Figure 14. Averaged particle number density at $x/D = 2$

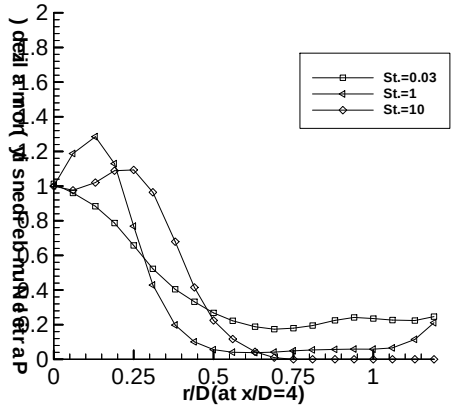

Figure 15. Averaged particle number density at $x/D = 2$

To further understand the dispersion process, time averaged particle number density profiles are presented in Figures 14 and 15. The averaged particle number density is normalized by the particle number density at the centerline, for the given axial location. At both $x = 2D$ and $x = 4D$, a peak value which is greater than 1 is observed between centerline and jet edge ($r = 0.5D$) for particles with Stokes numbers greater than 1.

5.3. Statistical results. Second moments. The turbulent stresses of the fluid and particle phases together with fluid-particle correlations play an important role in understanding the interaction between the phases. We denote by <> the (ensemble) averaging operator that is related to the particle phase.

Figures 16 and 17 depict the correlation between the fluid- and particle-fluctuations as well as the corresponding fluid Reynolds stresses at two different axial positions. For particles with Stokes number of 10 the absolute values of the fluid-particle cor-

relations are almost always smaller than the corresponding fluid turbulent Reynolds stresses, while for particles with Stokes number of 1, the absolute value of fluid-particle correlations may be higher than the corresponding fluid Reynolds stresses (Figure 17).

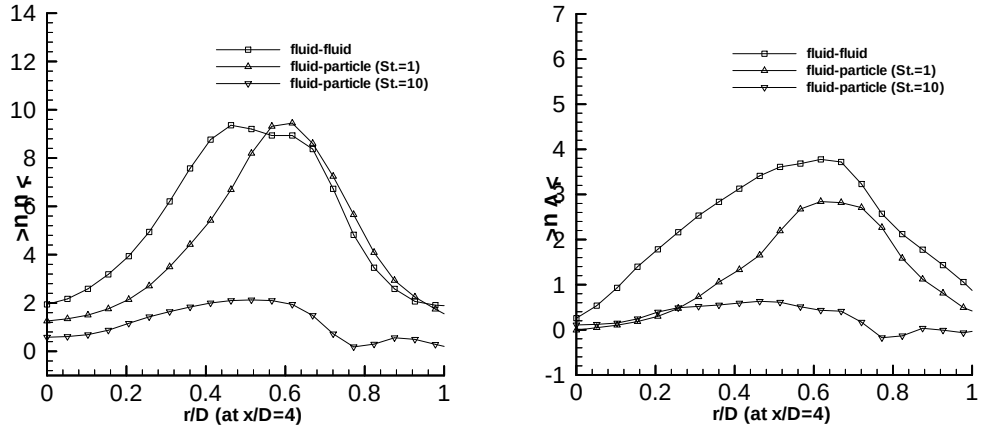

Figure 16. Fluid-particle, axial-axial (left) and axial-radial (right), correlations

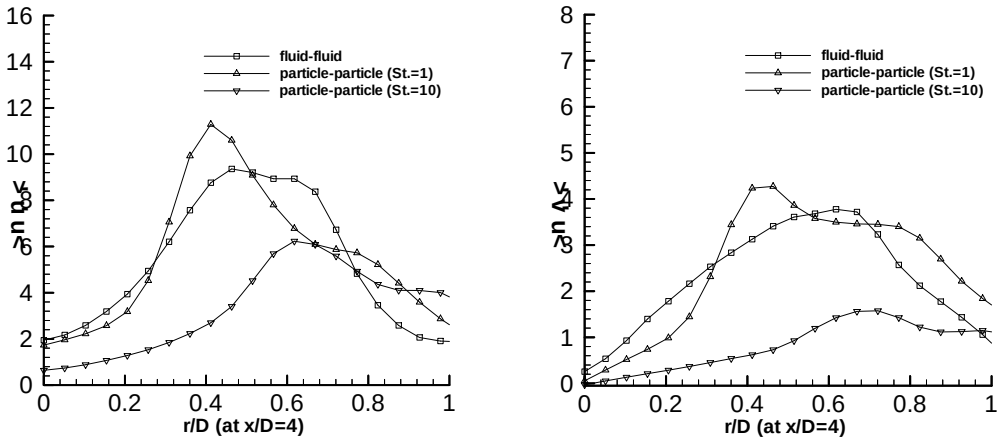

Figure 17. Particle phase Reynolds-stresses at $x/D = 4$

Figure 17 depicts the particle phase Reynolds-stresses at axial position of x/D=4. For both particles with Stokes numbers of 1 and 10, particle Reynolds-stresses may exceed the corresponding fluid turbulent Reynolds stress at certain radial positions. This means that particle turbulent properties are not only determined by their response to the fluid turbulent properties. We note that in this case the particles are not released at the fluid velocity at the jet nozzle. The inertia effect of the particles and

the particle initial conditions also play an important role in the turbulence properties of the particles. It is worth mentioning that Simonin [11] also found that the absolute value of particle Reynolds-stresses may be higher than the corresponding fluid turbulent Reynolds-stresses. Simonin [11] considered particle dispersion in turbulent shear flows. He attributed this to the existence of mean velocity gradients.

6. Concluding remarks

Unforced and forced jets loaded with heavy particles have been studied by Large Eddy Simulations. The combination with a Lagrangian Particle Tracking approach allows one to take into account the non-linear interactions between the phases. The numerical calculations have been compared with experimental data. Thus, the accuracy of the simulations in terms of mean and second moments has been established. The role of particle initial velocity for the dispersion process has been considered. For particles with Stokes numbers less than one, the initial velocity does not have much effect on the particle dispersion process. For particles with Stokes number of 10, different initial velocities may have a great effect on the dispersion process. We note that the larger the lag between the fluid velocity and particle velocity, the further downstream the dispersion may be observed. Quantitative analysis shows that particles are not only ejected away from the centerline of the jet, but also convected toward the jet axis. Due to this effect the particle number density distribution in the jet varies non-monotonously especially for particles with Stokes number around unity.

Acknowledgement. We would like to acknowledge the help of Dr. Jonas Bolinder with the experiments. This work was supported partially by STEM, the Swedish National Energy Administration and by the Foundation for Swedish Strategic through the "multi-phase flow" program. The financial support is highly appreciated.

REFERENCES

1. Longmire, E. K. and Eaton, J. K.: *Structure of a particle-laden round jet*, J. Fluid Mech., **236**, (1992), 217-257.
2. Kiger, K.T. and Lashearas, J.C.: *The effect of vortex paring on particle dispersion and kinetic energy transfer in a two-phase turbulent shear layer*, J. Fluid Mech., **302**, (1995), 149–178.
3. Squires, K.D. and Eaton, J.K.: *Preferential concentration of particles by turbulence*, Phys. Fluids, **3**(5), (1991), 928-937.
4. Chung, J.N. and Troutt, T.R.: *Simulation of particle dispersion in an axisymmetric jet*, J. Fluid Mech., **186**, (1988),199-222.
5. Uijttewaal, W.S.J. and Oliemans, R.V.A.: *Handling complex boundaries on a Cartesian grid using surface singularities,* To appear in J. Num. Meth. in Fluids, 2000.
6. Marcu, B. and Meiburg, E.: *The effect of streamwise braid vortices on the particle dispersion in a plane mixing layer. I. Equilibrium points and their stability*, Physics of Fluids, **8**, (1996), 715-753.
7. Tang, L., Wen, F., Yang, Y., Crowe, C. T., Chung, J. N. and Troutt, T. R.: *Self-organizing particle dispersion mechanism in a plane wake*, Phys. Fluids A, 4,

(1992), 2244-2250.

8. Gullbrand, J. and Fuchs, L.: *A comparative study of sub-grid scale models for a co-annular swirling jet.* Submitted for publication, 2001.
9. Maxey, M. R. and Riley, J. J.: *Equation of motion for a small rigid sphere in a nonuniform flow*, Phys. Fluids, **26**, (1983), 883-889.
10. Gullbrand, J., Bai, X.S. and Fuchs, L.: *High order Cartesian grid method for calculation of turbulent flows.* To appear in Int. J. Num. Meth. in Fluids. 2000.
11. Simonin, O.: *Eulerian Formulation for Particle Dispersion in Turbulent Two-phase Flows, in 5th Workshop on Two-phase Flow Predictions*, Eds. M. Sommerfeld and D. Wennerberg, Forschungszentrum Julich GmbH, ISBN 3-89336-066-2, (1990), 156-166.